Efficiently increasing the radiative rate of TADF material with metal coordination

Xian-Bao Cai,[a,b] DongLiang,[b] MingXue Yang,[b] Xiao-Yuan Wu,[b] Can-Zhong Lu*[abc] and Rongmin Yu*[ab]

a.College of Chemical Engineering, Fuzhou, University, 350116, Fuzhou, P. R. China.

b.CAS Key Laboratory of Design and Assembly of Functional Nanostructures, and Fujian Key Laboratory of Nanomaterials, Fujian Institute of Research on the Structure of Matter, Chinese Academy of Sciences, Fuzhou, Fujian, 350002, China.

c.University of Chinese Academy of Sciences, Beijing 100049, China.

EXPERIMENTAL SECTION. General Procedures. All reactions were carried out under the nitrogen atmosphere unless specified. Chemicals were purchased from commercial sources and used without further purification. The solvent were freshly distilled on suitable dry reagents. ^{1}H NMR and ^{13}C NMR spectra were recorded on a Bruker AVANCE III 400 MHz NMR spectrometer. Elemental analyses (C, H, N) were carried out with an Elementar Vario EL III elemental analyzer. TGA and differential scanning calorimetry (DSC) of samples were performed on a METTLER TOLEDO TGA/DSC 1 STARe System with a heating rate of 10 ºC/min under nitrogen. UV–vis absorption spectra were recorded with a PerkinElmer LAMBDA 650 UV-vis spectrometer. PL spectra of solution, film and solid samples were carried out with an Edinburgh FLS980 fluorescence spectrometer. The transient PL characteristics of solid and solution samples were performed on an Edinburgh analytical instrument FLS980 with a picosecond laser diode. The PL quantum yields of film and solid samples were defined as the number of photons emitted per photon absorbed by the systems and measured by an Edinburgh FLS1000 spectrofluorophotometer. And the variable-temperature measurements were carried out on corresponding instruments by using an additional LINKAM THMS600 system.

Synthesis of 2,3,5,6-tetrafluoro-4-(3-(pyridin-2-yl)-1H-pyrazol-1-yl)benzonitrile. To a solution of 2-(1H-pyrazol-3-yl)pyridine (1.0 mmol, 145 mg) in dry THF (5 mL) were added K_2CO_3 (2.0 mmol, 272 mg) and pentafluorobenzonitrile (1.0 mmol, 193 mg). The reaction mixture was refluxed for 12 h at 90°C in an oil bath. When it is cool, the solvent was removed by vacuum-rotary evaporation. The residue was extracted with CH_2Cl_2. The extract was washed with brine and dried using anhydrous sodium sulfate. The product as a white solid was obtained by column chromatography on silica gel (251.2 mg, 80%). ^{1}H NMR (400 MHz, DMSO-d6) δ 8.67 (s, 1H), 8.39 (s, 1H), 8.14-7.73 (m, 2H), 7.43 (s, 1H), 7.25 (s, 1H).

Synthesis of TCzBN-PyPz. To a solution of 9H-carbazole (4.2 mmol, 701 mg) was added to a suspension of NaH (60% in mineral oil 336 mg, 8.4 mmol) in anhydrous THF (10 ml) at 0 °C. After stirring under Ar for 30 min, 2,3,5,6-tetrafluoro-4-(3-(pyridin-2-yl)-1H-pyrazol-1-yl)benzonitrile (314 mg, 1.0 mmol) was added. After stirred overnight, the reaction mixture was cooled to room temperature and quenched with water (50 ml). The resulting precipitate was filtered and washed with water. The product as a greenish yellow powder was obtained by column chromatography

on silica gel (453 mg, 50%). ^{1}H NMR (400 MHz, DMSO-d6) δ 8.17 (d, J = 4.8 Hz, 1H), 7.94 (dd, J = 11.0, 8.0 Hz, 7H), 7.79 (d, J = 8.2 Hz, 4H), 7.71 (d, J = 7.7 Hz, 4H), 7.32 – 7.20 (m, 5H), 7.17 – 7.02 (m, 9H), 6.98 (t, J = 7.4 Hz, 4H), 6.52 (d, J = 2.0 Hz, 1H), 5.93 (d, J = 8.0 Hz, 1H), 5.84 (d, J = 2.0 Hz, 1H). ^{13}C NMR (101 MHz, DMSO-d6) δ 152.34, 149.88, 148.53, 144.79, 142.15, 139.93, 139.74, 135.87, 135.17, 130.83, 125.45, 124.94, 122.91, 122.82, 120.75, 120.29, 120.13, 119.70, 119.13, 117.45, 112.42, 111.32, 110.94, 105.28. Anal. Calcd for $C_{63}H_{38}N_8$: C, 83.35; H, 4.19; N, 12.35. Found: C, 83.50; H, 4.13; N, 12.34.

Synthesis of Complex 1. A mixture of TCzBN-PyPz (0.1 mmol) and $P(Ph)_2CH_3$ (0.1 mmol) in CH_2Cl_2 (10 ml) was stirred for 30 min at room temperature, and then $[Ag(CH_3CN)_4]BF_4$ (0.1 mmol) was added. After the mixture was stirred for 1 hour, the solvent was removed by evaporation. The residue was extracted with CH_2Cl_2. The product as crystalline solid was obtained from a diffusion of ether into the above CH_2Cl_2 solution overnight. Yield (33%). $[Ag(PPh_2CH_3)(TCzBN\text{-}PyPz)]BF_4$ (**1**). Anal. Calcd for $C_{76}H_{51}AgBF_4N_8P$: C, 70.06; H, 3.92; N, 8.60. Found: C, 69.16; H, 3.98; N, 8.71.

X-ray Crystallographic Analysis. Diffraction data for TCzBN-PyPz was collected on a SuperNova, Dual, Cu at zero, Atlas diffractometer equipped with graphite-monochromated Cu Kα radiation (λ=1.54184 Å). The measurement for **1** was made by using graphic monochromatic Mo Kα radiation (λ=0.71073 Å). Structures were solved by direct methods and refined by full-matrix least-squares methods using the SHELXL-97 program package.[1] Hydrogen atoms were added in idealized positions. All nonhydrogen atoms were refined anisotropically. Details of the crystal and structure refinements are listed in **Table S1**. Selected bond lengths and bond angles are listed in **Table S2**. CCDC 2172221 and 2172222 contain the supplementary crystallographic data for complexes TCzBN-PyPz and **1**, respectively.

The average of the dihedral angles between the carbazole planes and benzonitrile core is 71.6 and 71.3° for the free ligand and complex **1**, respectively. The dihedral angle between the pyrazole group and the benzonitrile core is 73.93(5)° and 70.9(2)° for the free ligand and complex **1**, respectively. The pyrazole group and the pyridyl group are nearly coplanar in complex **1**, while are not coplanar in the free ligand. The dihedral angle between the pyrazole group and the pyridyl group is 3.0(2)° and 30.40(5)° in complex **1** and the free ligand , respectively.

Table S1. Selected crystallographic data of complex **1** and TCzBN-PyPz.

Compound reference	**1**	TCzBN-PyPz
Chemical formula	$C_{77}H_{53}AgBCl_2F_4N_8P$	$C_{63}H_{38}N_8$
Formula Mass	1386.82	907.01
Temperature/K	100.0(3)	100.00(13)
Crystal system	monoclinic	monoclinic
Space group	Cc	$P2_1/n$
a/Å	13.7000(8)	15.3086(5)
b/Å	24.3133(11)	11.2453(4)
c/Å	19.1731(8)	26.5143(10)
α/º	90	90
β/º	93.799(5)	93.018(3)
γ/º	90	90

Volume/Å^3	6372.4(5)	4558.1(3)
Z	4	4
ρ_{calc} g/cm^3	1.446	1.322
μ/mm^{-1}	0.490	0.621
F(000)	2832.0	1888.0
Crystal size/mm^3	0.2 × 0.15 × 0.05	0.4 × 0.3 × 0.2
Radiation	Mo Kα (λ = 0.71073)	Cu Kα (λ =1.541)
Reflections collected	17085	19411
Independent reflections	11202 [R_{int} = 0.0638, R_{sigma} = 0.0926]	9135 [R_{int} = 0.0282, R_{sigma} = 0.0299]
Data/restraints/parameters	11202/2/848	9135/0/640
Goodness-of-fit on F^2	1.059	1.047
Final R indexes[I>=2σ (I)]	R_1 = 0.0591, wR_2 = 0.1423	R_1 = 0.0416, wR_2 = 0.1044
Final R indexes [all data]	R1 = 0.0688, wR2 = 0.1565	R_1 = 0.0499, wR_2 = 0.1110
Largest diff. peak/hole / e Å-3	1.24/-0.90	0.20/-0.29

[a]R_1=∑||Fo| - |Fc|| /∑|Fo|. [b]wR_2=[∑w(Fo^2_ Fc^2)^2/∑w(Fo^2)]$^{1/2}$

Table S2. Selected bond distances (Å) and angles (º) of complex **1**.

Compound		**1**
Distances(Å)	Ag1-N7	2.311(5)
	Ag1-N8	2.298(6)
	Ag1-P1	2.3547(17)
Angles(º)	N7-Ag1-N8	72.2(2)
	N8-Ag1-P1	130.90(15)
	N7-Ag1-P1	147.18(14)

Thermogravimetric analysis.

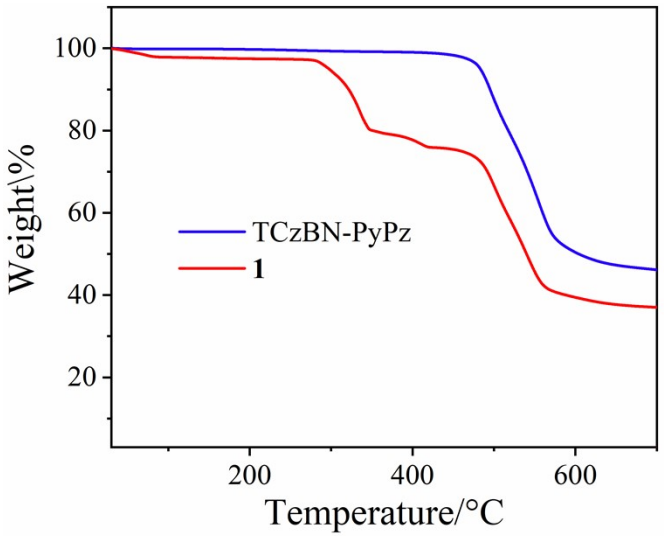

Fig. S1 Thermogravimetric analysis curves of TCzBN-PyPz and **1**.

Electrochemical measurements. Cyclic voltammetry was performed in a gastight single-compartment three-electrode cell with a CHI604E Voltammetric Analyzer at room temperature. A glassy carbon disk and a platinum wire were selected as the working and auxiliary electrodes, respectively. The reference electrode was Ag/Ag+ (0.01 M of AgNO3 in acetonitrile). The CV measurements were carried out in anhydrous and nitrogen-saturated acetonitrile solutions with 0.1 M n-tetrabutylammonium hexafluorophosphate and 2.0 mM investigated compounds. The ferrocenium/ferrocene couple was used as an internal standard.

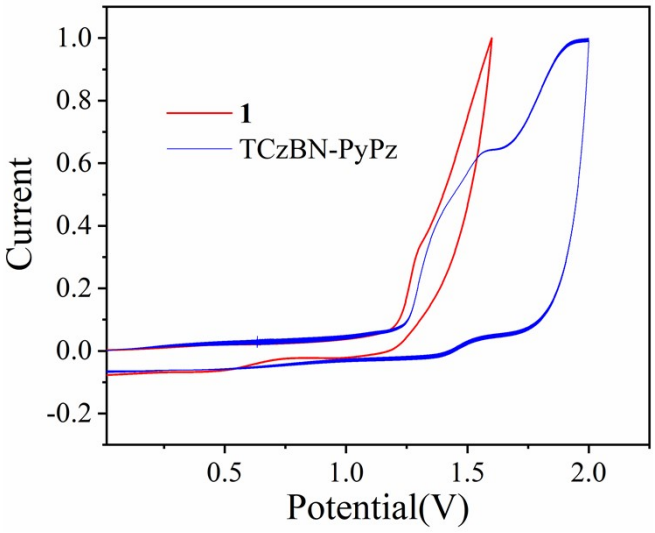

Fig. S2 Cyclic voltammogram of complex **1** and TCzBN-PyPz in degassed acetonitrile.

Theoretical Calculations. All the calculations were carried out using the Gaussian 09 program package.[2] The density functional theory (DFT) and time-dependent density functional theory(TD-DFT) calculations were performed at PBE0 level in conjunction with the polarizable continuum model (PCM) using dichloromethane as the solvent.[3-7] The structure in the singlet ground (S_0) was optimized via DFT. The S_1 and T_1 geometries were optimized via TDDFT. The input coordinates were extracted from the X-ray crystallographic data. In all calculations, the relativistic effective core potential (RECP) and the associated basis set Lanl08(f) and Lanl08(d), which are the revised version of the original Hay-Wadt basis set, were employed for Ag(I) atoms.[8] An all-electron basis set of 6-31G* was used for P, C, N and H.[9] Visualization of the optimized structures and frontier molecular orbitals were performed with GaussView. The partition orbital compositions were analyzed by the Multiwfn 2.4 program.[10]

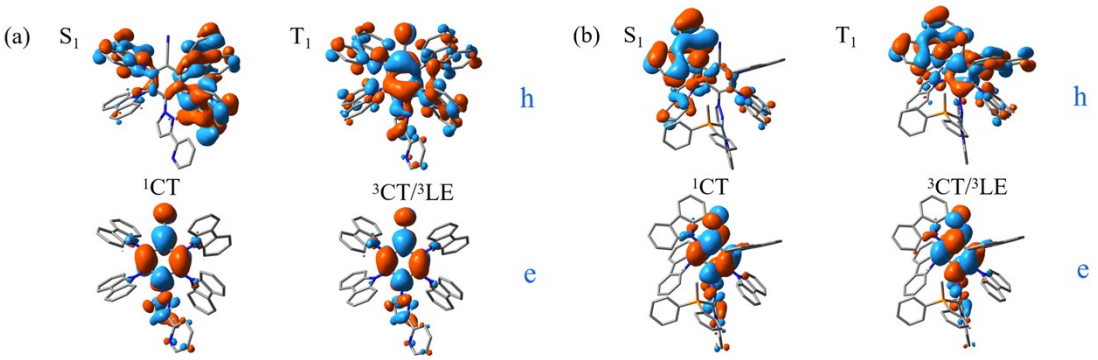

Fig. S3 (a) NTO pairs for S_1 and T_1 states of TCzBN-PyPz in the optimized S_0 structure. (b) NTO pairs for S_1 and T_1 states of complex **1** in the optimized S_0 structure.

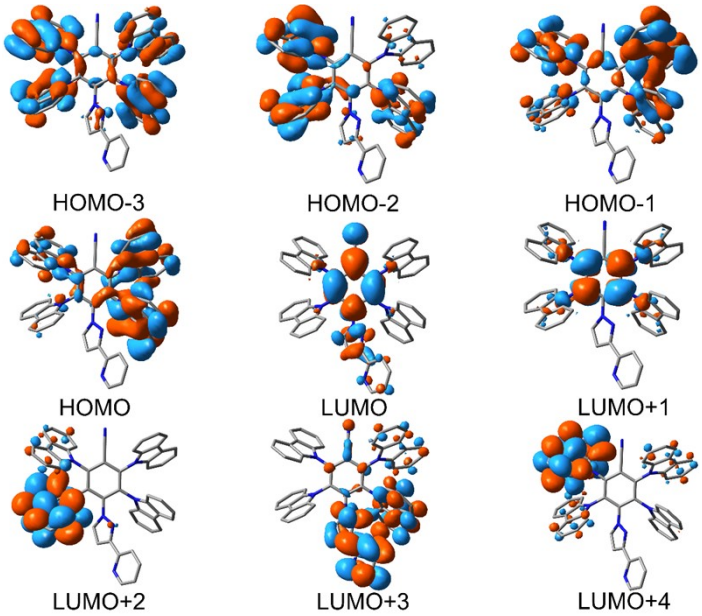

Fig. S4 Frontier orbitals from HOMO-3 to LUMO+4 of TCzBN-PyPz in the optimized S_0 structure.

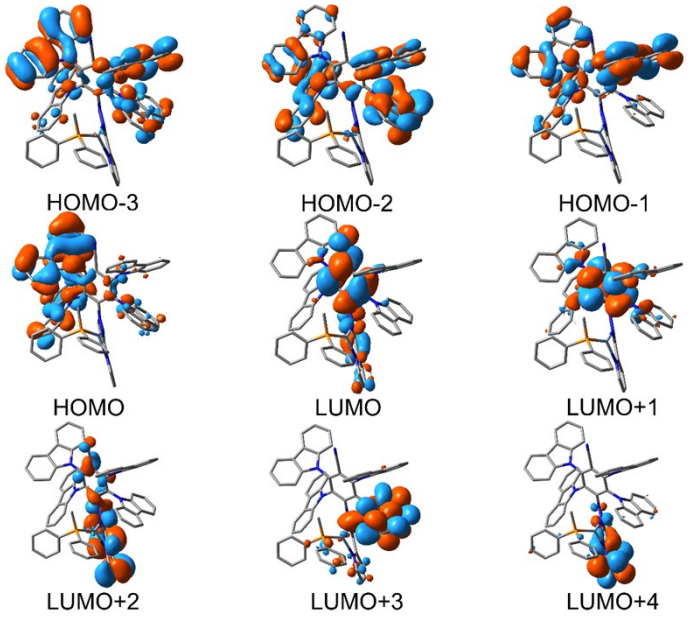

Fig. S5 Frontier orbitals from HOMO-3 to LUMO+4 of **1** in the optimized S_0 structure.

Table S3. Composition of HOMO-3 - LUMO+4 of complex **1** and TCzBN-PyPz in the optimized S_0 structure.

		Energy (eV)	Ag	Cz	PN-PyPz	P(Ph)3
	HOMO-3	-6.5050	0.53251 %	90.21904 %	7.28308 %	0.85050 %
	HOMO-2	-6.3860	1.10609 %	87.78150 %	7.10286 %	1.17519 %
	HOMO-1	-6.3308	0.08691 %	90.63537 %	7.44402 %	0.16679 %
	HOMO	-6.2886	0.18457 %	87.30613 %	10.86892 %	0.28484 %
1	LUMO	-2.7533	0.20663 %	11.24481 %	88.40747 %	0.07131 %
	LUMO+1	-2.1196	0.20175 %	25.24049 %	74.31985 %	0.13051 %
	LUMO+2	-1.9071	2.89204 %	2.56076 %	92.62604 %	1.91564 %

	LUMO+3	-1.3138	5.07057 %	80.48299 %	6.26623 %	8.17981 %
	LUMO+4	-1.1834	2.02444 %	4.45150 %	88.80686 %	4.71059 %
				Cz	PN-PyPz	
	HOMO-3	-6.0741		88.89200 %	11.10800 %	
	HOMO-2	-5.9224		89.97430 %	10.02570 %	
	HOMO-1	-5.8827		92.67855 %	7.32145 %	
	HOMO	-5.8405		88.41721 %	11.58279 %	
TCzBN-PyPz	LUMO	-2.1485		12.50986 %	87.49014 %	
	LUMO+1	-1.6199		25.85363 %	74.14637 %	
	LUMO+2	-0.7941		95.24635 %	4.75365 %	
	LUMO+3	-0.7580		29.95369 %	70.04631 %	
	LUMO+4	-0.6990		95.55622 %	4.44378 %	

Table S4. Calculated energy levels, and orbital transition analyses for TCzBN-PyPz, and complex **1** in the optimized S_0 geometries at the PBE0/6-31G*/LANL2DZ Levels.

complexes	states	Energy (eV)	λ_{cal} (nm)	Main contributions	ILCT	ILLE
	S_1	2.8996	427.6	H→L(97.4157%)	75.02%	24.98%
	T_1	2.6517	467.9	H-1→L(43.9622%) H→L+1(9.9066%)	44.99%	55.01%
TCzBN-PyPz	T_2	2.7708	447.7	H→L(84.4714%) H-2→L(5.3282%)	69.27%	30.73%
	T_3	2.8800	430.6	H-2→L(63.1373%) H-1→L(21.9082%)	71.32%	28.68%
	S_1	2.7425	452.1	H→L(91.4601%) H-1→L(5.3021%)	76.57%	11.66%
	T_1	2.5882	479.1	H-1→L(54.3195%) H→L(11.0497%) H-2→L(8.5582%)	63.66%	25.17%
1	T_2	2.6368	470.3	H→L(78.25%) H-1→L(14.1682%)	69.25%	19.27%

Table S5. Compositions of hole and electron for the S_1 states of TCzBN-PyPz, complex **1** in the optimized S_0 structure.

		Ag	Cz	PN-PyPz	phosphine ligands
	Hole	0.16266%	88.13565%	11.05443%	0.21522%
1	electron	0.10903%	11.56081%	88.23736%	0.04144%
	difference	0.05363%	76.57484%	-77.18293%	-0.17378%
	Hole		87.52527%	12.47473%	
TCzBN-PyPz	electron		12.50838%	87.49162%	
	difference		75.01689%	-75.01689%	

Table S6. Compositions of hole and electron for the T_1 states of TCzBN-PyPz, complex **1** in the optimized S_0 structure.

		Ag	Cz	PN-PyPz	phosphine ligands
1	Hole	0.20835%	74.66118%	24.04084%	0.23803%
	electron	0.08314%	11.00317%	88.83513%	0.02806%
	difference	0.12521%	63.65801%	-64.79429%	0.20997%
TCzBN-PyPz	Hole		55.79027%	44.20973%	
	electron		10.79955%	89.20045%	
	difference		44.99072%	-44.99072%	

Photophysical Measurements.

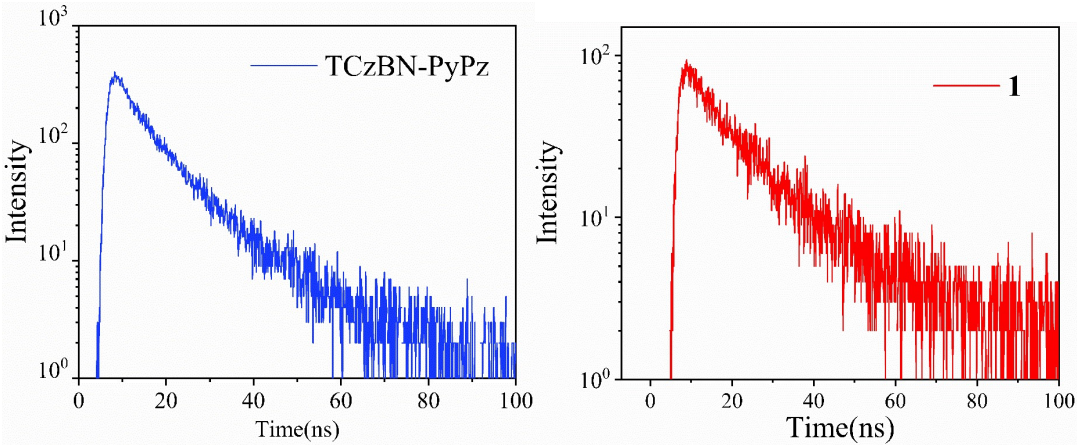

Fig. S6 Transient PL decay spectra of **1** and TCzBN-PyPz in solid state at 298K.

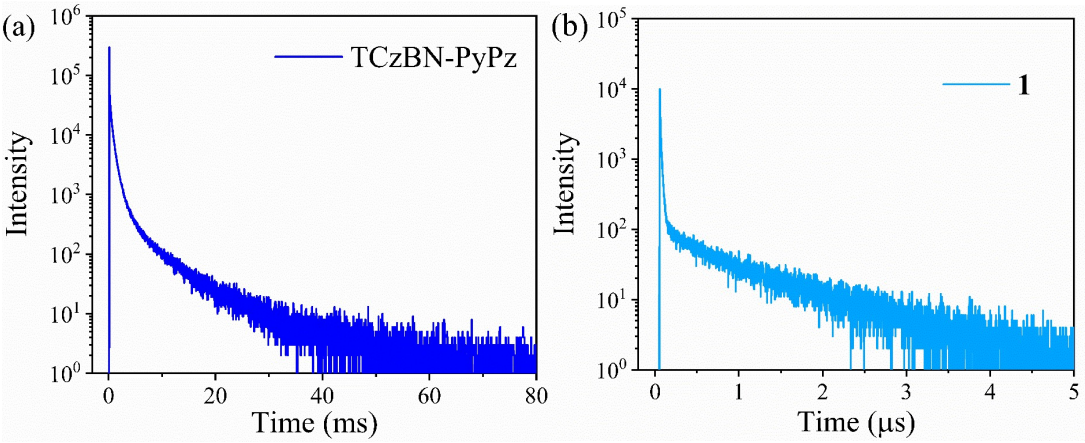

Fig. S7 Transient PL decay spectra of **1** and TCzBN-PyPz in solid state at 298K.

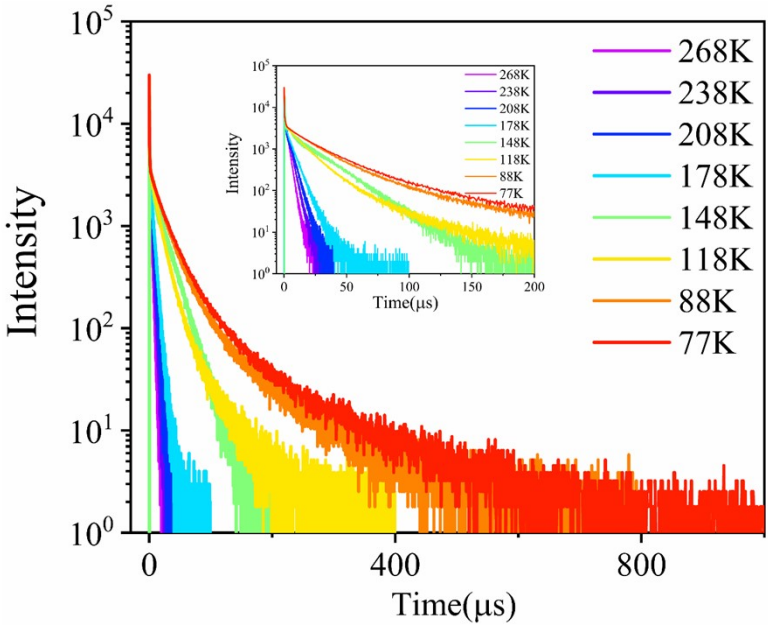

Fig. S8 Temperature-dependent transient PL decay curves of **1** at temperatures ranging from 77 to 268 K. Inset: transient PL decay curves of **1** at time ranging from 0 to 200 μs.

NMR spectra.

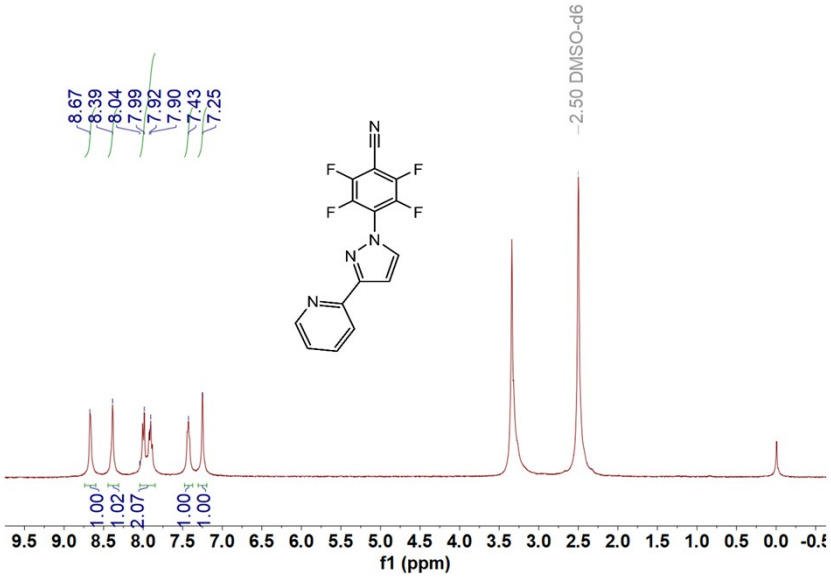

Fig. S9 ^{1}H NMR spectrum of 2,3,5,6-tetrafluoro-4-(3-(pyridin-2-yl)-1H-pyrazol-1-yl)benzonitrile in DMSO-d6.

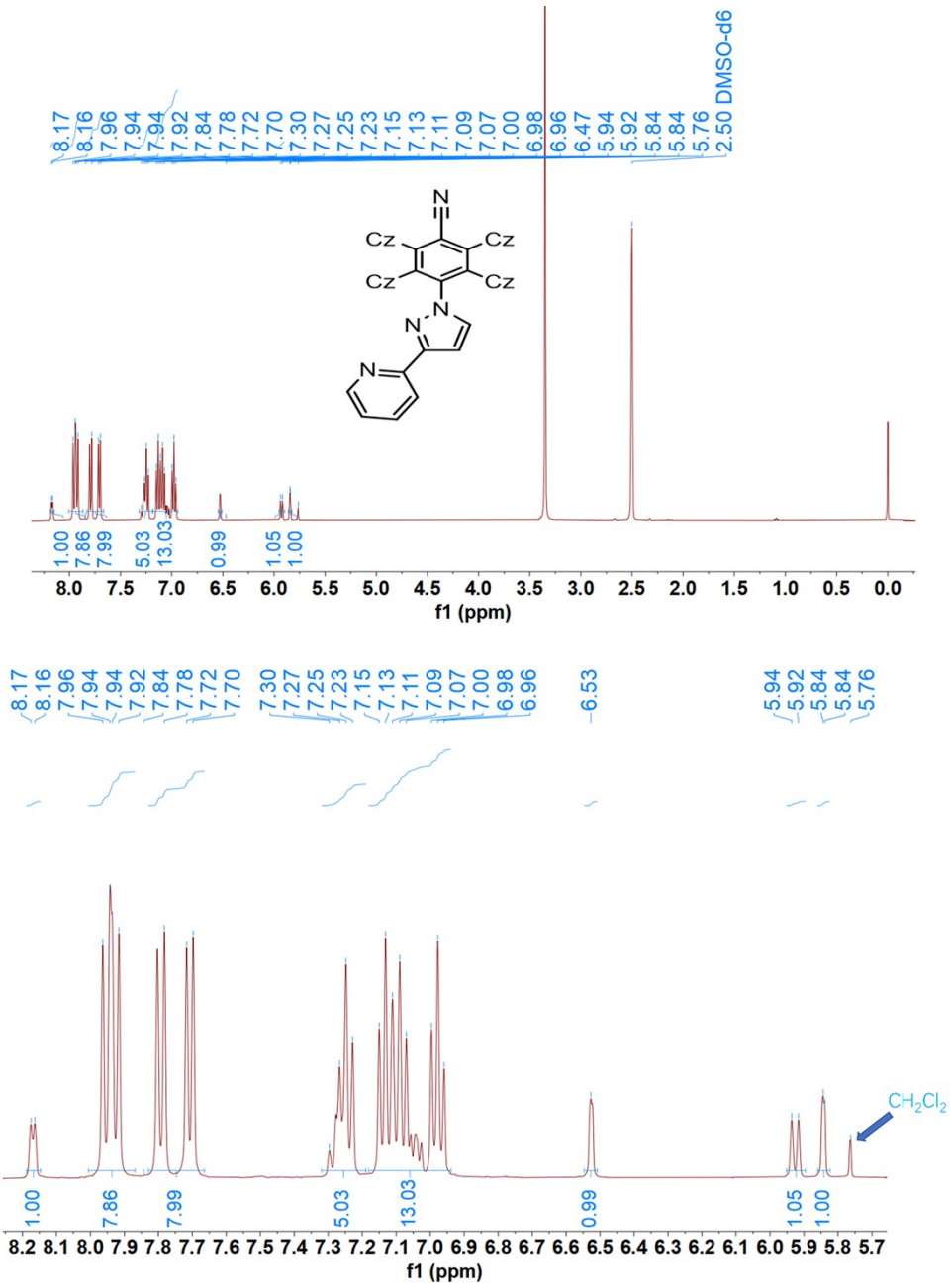

Fig. S10 ^{1}H NMR spectrum of 2,3,5,6-tetra(9H-carbazol-9-yl)-4-(3-(pyridin-2-yl)-1H-pyrazol-1-yl)enzonitrile (TCzBN-PyPz) in DMSO-d6.

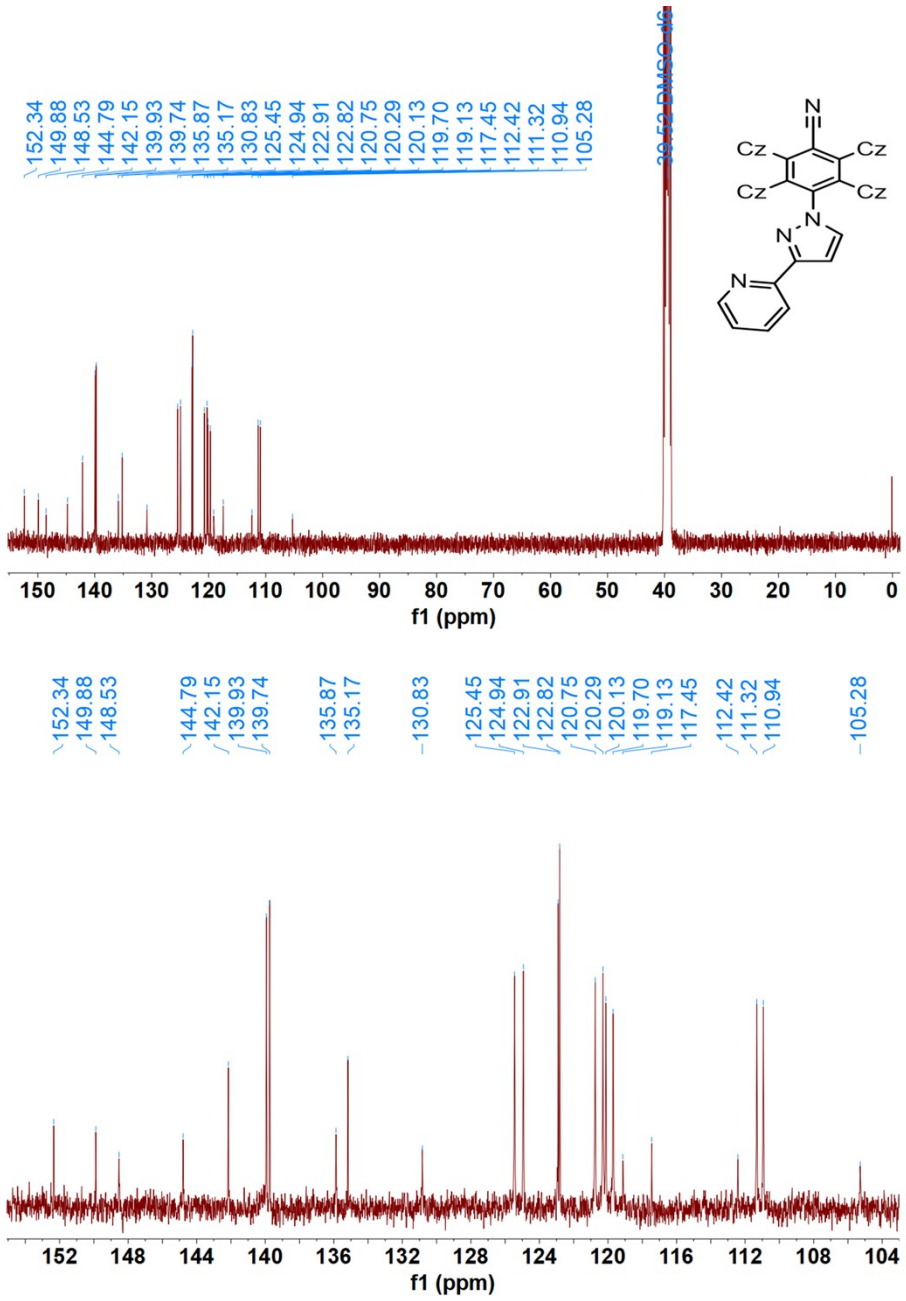

Fig. S11 ^{13}C NMR spectrum of 2,3,5,6-tetra(9H-carbazol-9-yl)-4-(3-(pyridin-2-yl)-1H-pyrazol-1-yl)enzonitrile (TCzBN-PyPz) in DMSO-d6.

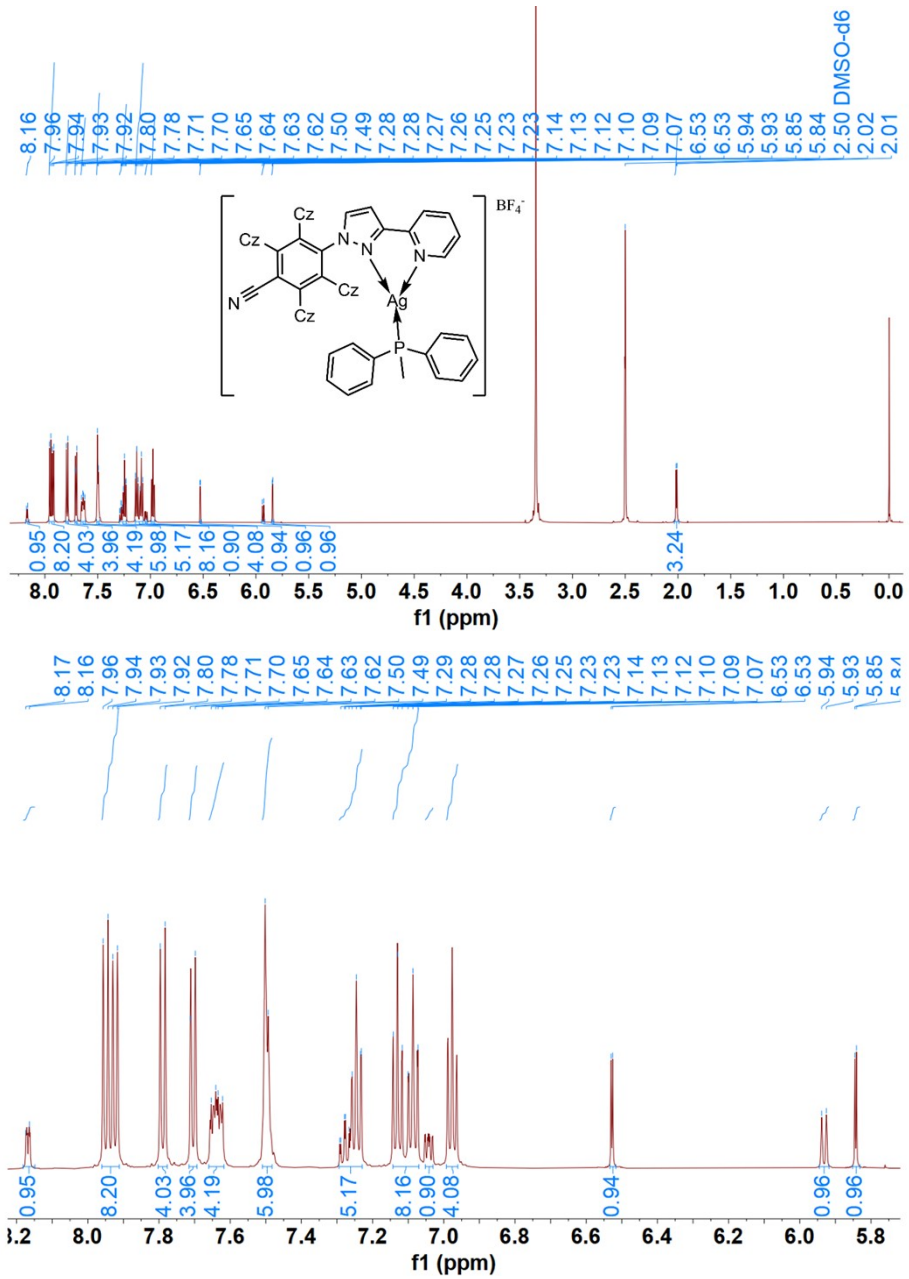

Fig. S12 ^{1}H NMR spectrum of complex **1** in DMSO-d6.

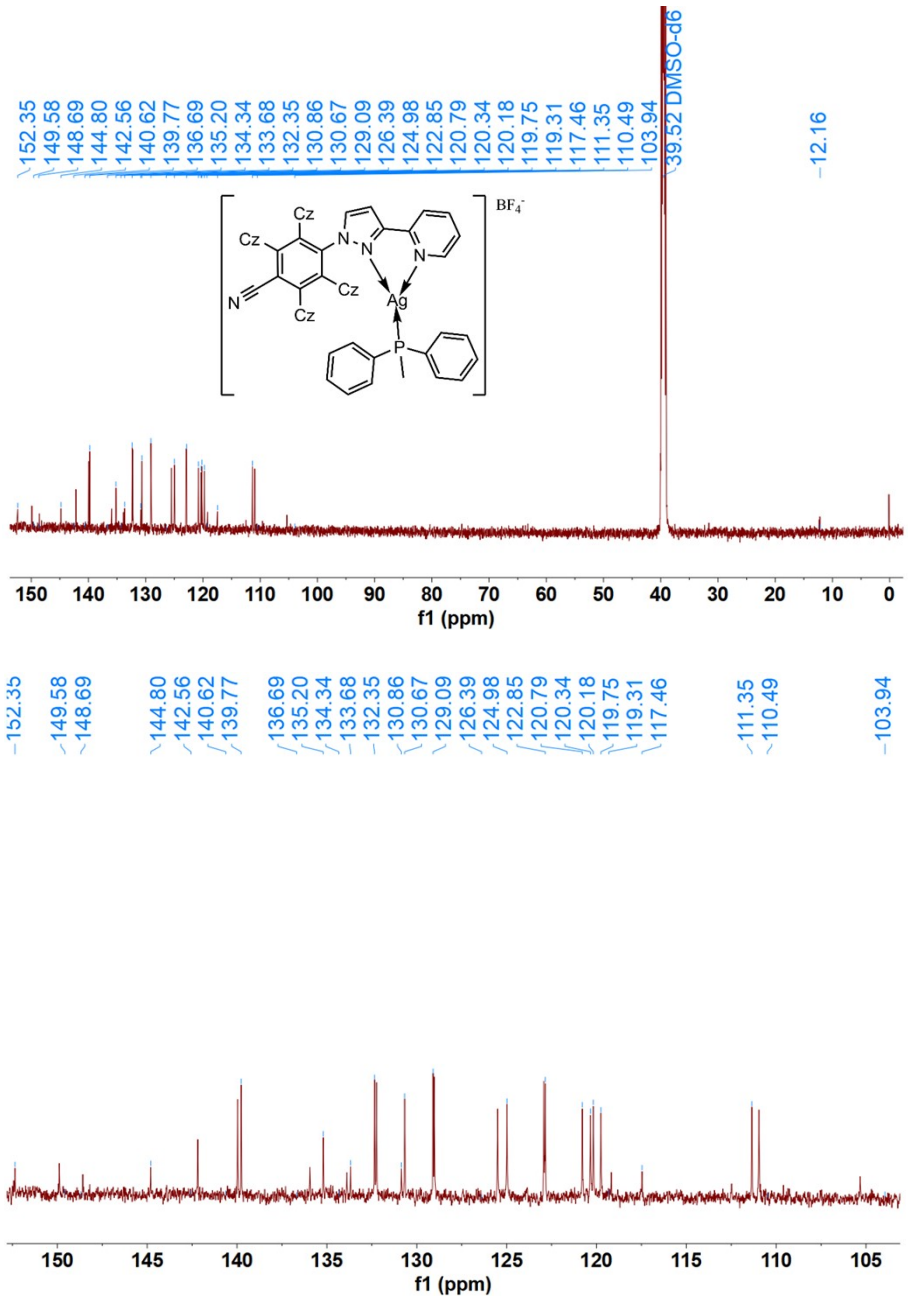

Fig. S13 ^{13}C NMR spectrum of complex **1** in DMSO-d6.

Mass spectra.

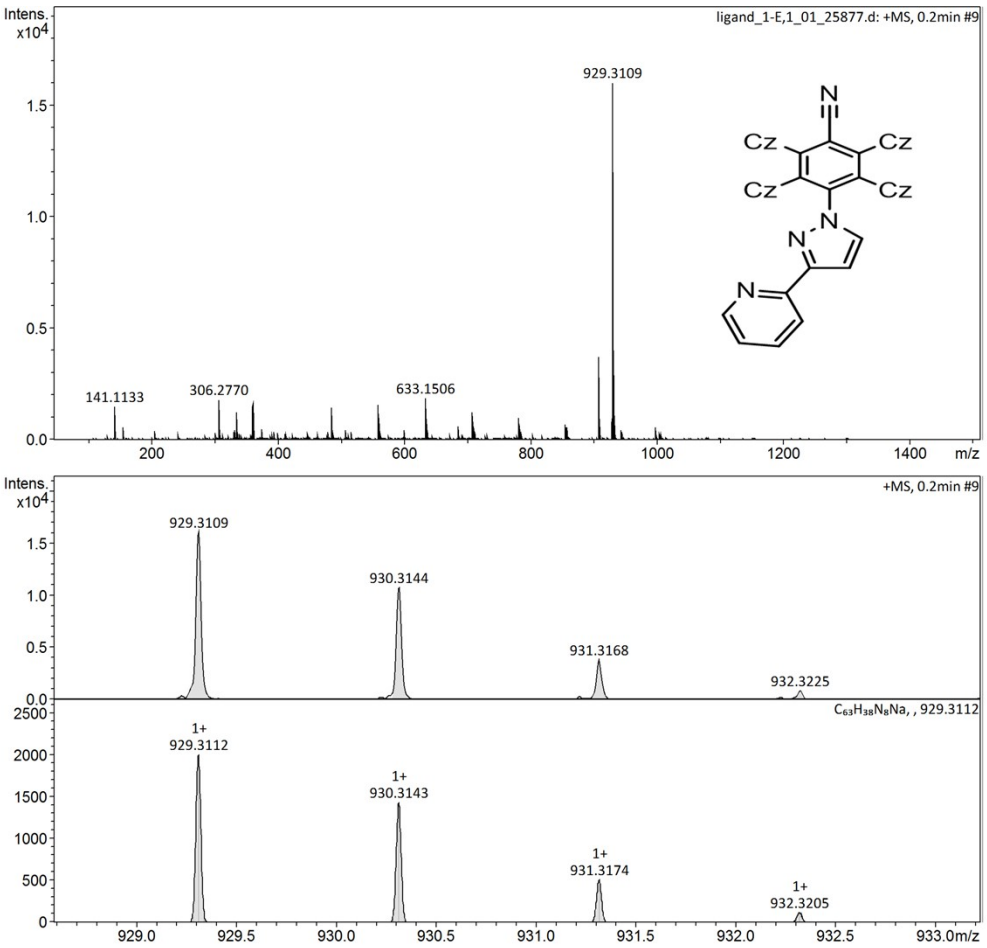

Fig. S14 Mass spectra of TCzBN-PyPz.

Reference.

(1) Sheldrick, G. M. SHELXS-2014/7 and SHELXL-2014/7 Program for Solution and Refinement of Crystal Structures; Institute forInorganic Chemistry, University of Göttingen: Göttingen, Germany, 2014.

(2) Frisch, M. J.; Trucks, G. W.; Schlegel, H. B.; Scuseria, G. E.; Robb, M. A.; Cheeseman, J. R.; Scalmani, G.;Barone, V.; Mennucci, B.; Petersson, G. A.; Nakatsuji, H.; Caricato, M.; Li, X.; Hratchian, H. P.; Izmaylov, A. F.;Bloino, J.; Zheng, G.; Sonnenberg, J. L.; Hada, M.; Ehara, M.; Toyota, K.; Fukuda, R.; Hasegawa, J.; Ishida, M.;Nakajima, T.; Honda, Y.; Kitao, O.; Nakai, H.; Vreven, T.; Montgomery Jr., J. A.; Peralta, J. E.; Ogliaro, F.;Bearpark, M.; Heyd, J. J.; Brothers, E.; Kudin, K. N.; Staroverov, V. N.; Keith, T.; Kobayashi, R.; Normand, J.;Raghavachari, K.; Rendell, A.; Burant, J. C.; Iyengar, S. S.; Tomasi, J.; Cossi, M.; Rega, N.; Millam, J. M.; Klene, M.; Knox, J. E.; Cross, J. B.; Bakken, V.; Adamo, C.; Jaramillo, J.; Gomperts, R.; Stratmann, R. E.; Yazyev, O.; Austin, A. J.; Cammi, R.; Pomelli, C.; Ochterski, J. W.; Martin, R. L.; Morokuma, K.; Zakrzewski, V. G.; Voth, G. A.; Salvador, P.; Dannenberg, J. J.; Dapprich, S.; Daniels, A. D.; Farkas, O.; Foresman, J. B.; Ortiz, J. V.; Cioslowski J.; and Fox, D. J.; Gaussian 09, Revision D.01; Gaussian, Inc., Wallingford, CT, 2009.

(3) Adamo, C.; Barone, V. Toward reliable density functional methods without adjustable parameters: The PBE0 model. J. chem. Phys. 1999, 110, 6158-6170.

(4) Perdew, J. P. Ernzerhof M, Burke K. Rationale for mixing exact exchange with density functional approximations. J. chem. Phys. 1996, 105, 9982-9985.

(5) Cances, E.; Mennucci, B.; Tomasi, J. A new integral equation formalism for the polarizable continuum model: Theoretical background and applications to isotropic and anisotropic dielectricsJ. J. chem. Phys.1997, 107, 3032-

3041.
(6) Mennucci, B.; Cancès, E.; Tomasi, J. Evaluation of Solvent Effects in Isotropic and Anisotropic Dielectrics and in Ionic Solutions with a Unified Integral Equation Method: Theoretical Bases, Computational Implementation, and Numerical Applications. J. Phys. Chem. B 1997, 101 (49), 10506-10517.
(7) Miertuš, S.; Scrocco, E.; Tomasi, J. Electrostatic interaction of a solute with a continuum. A direct utilizaion of AB initio molecular potentials for the prevision of solvent effects. Chem. Phys. 1981, 55, 117-129.
(8) Roy, L. E.; Hay, P. J.; Martin, R. L. Revised Basis Sets for the LANL Effective Core Potentials. J. Chem.Theory Comput. 2008, 4, 1029-1031.
(9) Hariharan, P. C.; Pople, J. A. Accuracy of AH n equilibrium geometries by single determinant molecular orbital theory Mol. Phys. 1974, 27,209-214.
(10) Lu, T.; Chen, F. Multiwfn: a multifunctional wavefunction analyzer. J. Comput. Chem. 2012, 33, 580-592.